How Penetrable Are Thioalkyl Self-Assembled Monolayers?

ARTICLE *in* JOURNAL OF PHYSICAL CHEMISTRY LETTERS · JULY 2010

Impact Factor: 7.46 · DOI: 10.1021/jz100587g

THE JOURNAL OF PHYSICAL CHEMISTRY Letters

pubs.acs.org/JPCL

How Penetrable Are Thioalkyl Self-Assembled Monolayers?

Carla Waring,[†] Paul A. J. Bagot,[†] Magnus W. P. Bebbington,[†] Minna T. Räisänen,[‡] Manfred Buck,[‡] Matthew L. Costen,[†] and Kenneth G. McKendrick*,[†]

[†]School of Engineering and Physical Sciences, Heriot-Watt University, Edinburgh EH14 4AS, U.K., and [‡]School of Chemistry, University of St. Andrews, St. Andrews, Fife KY16 9ST, U.K.

ABSTRACT The depth of penetration of photolytically generated, gas-phase $O(^3P)$ atoms into thioalkyl self-assembled monolayers (SAMs) has been investigated. Custom-synthesized, site-selectively deuterated SAMs were prepared on Au substrates and characterized by scanning tunneling microscopy (STM). Relative yields of gas-phase OD were detected by laser-induced fluorescence (LIF). Reaction was suppressed at the terminal CD_3 by the higher abstraction barriers for primary D atoms, yielding only 16 ± 3% of the total OD. The C_2 (first secondary) site is the individually most reactive (42 ± 5%). The remaining significant contribution (42 ± 4%) from positions as deep as C_3−C_6 is a considerable surprise when compared with previous related experiments using higher-energy O^+ ion projectiles and detecting OH^- products. The apparent greater penetrability of the SAM layer found here may have prior theoretical support. Furthermore, we show that NO_2 damages the surfaces but that C_{12} SAMs are considerably more resistant than C_6 SAMs.

SECTION Surfaces, Interfaces, Catalysis

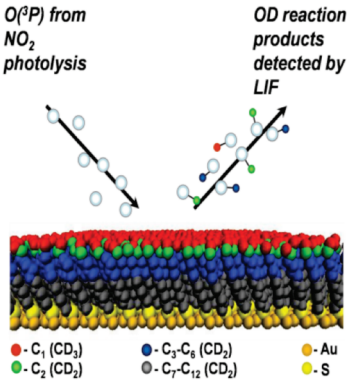

Self-assembled monolayers (SAMs) are of increasing importance in a wide range of potential applications, from lubrication to biotechnological devices. A thorough understanding of reactions at the gas−SAM interface holds the key to further progress in many of these areas. However, aside from a limited number of kinetic studies,[1−3] this reactivity remains poorly understood, particularly at a detailed dynamical level.[4−6]

The dynamics of nonreactive, inelastic collisions between (mostly) closed-shell species and SAMs have been more widely investigated using molecular beam techniques. The effects on energy exchange with the surface of scattering species, collision energy, SAM terminal group, and alkyl chain length have been studied.[7−12] The results mirror some aspects of related work at the gas−liquid interface.[13,14] Experimental scattering results are often empirically separable into apparent limiting "direct" (fast, impulsively scattered) and "thermal desorption" (relatively slow, Maxwellian at or near the surface temperature) components. Associated theoretical modeling has, however, highlighted that relatively slow-moving Boltzmann-like products cannot necessarily be uniquely associated with long-lived, trapping-type trajectories[15,16] Nevertheless, the extent to which the incoming projectile penetrates beyond the outermost layers of the surface is obviously a crucial factor affecting the probability of dissipative secondary encounters.

Although there have been a number of related studies of reactive species recently, particularly O and F atoms[17−31] with liquids, we believe that dynamical experimental studies of reactions at SAM surfaces have been restricted to our own preliminary work[32] with $O(^3P)$ and that of Jacobs[4−6] using much higher energy O^+ ions. Unlike inelastic scattering, where penetration depth can only be inferred indirectly,[7−12] reactive probes offer the possibility of reporting directly on the sites they are able to access. The Jacobs experiments are the only prior attempts to measure the depth of penetration into the SAM surface using isotopic labeling. They are therefore the only existing tests of this key aspect of theoretical attempts to model collisions of reactive projectiles with SAM layers.[33,34]

In the current work, we explore for the first time the accessibility of isotopically labeled sites in thioalkyl SAMs to gas-phase $O(^3P)$ atoms. The $O(^3P)$ is generated by 355 nm photolysis of NO_2,[35] resulting in a fairly broad, modestly superthermal laboratory-frame kinetic energy distribution (mean = 16 kJ mol^{-1}; fwhm = 26 kJ mol^{-1}). Only the more energetic of these $O(^3P)$ atoms are therefore able to abstract hydrogen atoms from alkyl chains, given the typical activation barriers of 34 and 22 kJ mol^{-1} for primary and secondary C−H bonds, respectively.[36] Reactions with SAM layers formed from two partially deuterated ($CD_3(CH_2)_{11}SH$ and $CD_3CD_2(CH_2)_{10}SH$) and two fully deuterated ($C_6D_{13}SH$ and $C_{12}D_{25}SH$) linear thiols were studied. The relative yields of gas-phase OD products were detected by laser-induced fluorescence (LIF). The structure and integrity of the SAM layers were monitored by supporting scanning tunneling microscopy (STM) measurements, including some corroborating measurements on undeuterated SAMs.

Received Date: May 7, 2010
Accepted Date: June 1, 2010
Published on Web Date: June 08, 2010

DOI: 10.1021/jz100587g | *J. Phys. Chem. Lett.* **2010**, *1*, 1917–1921

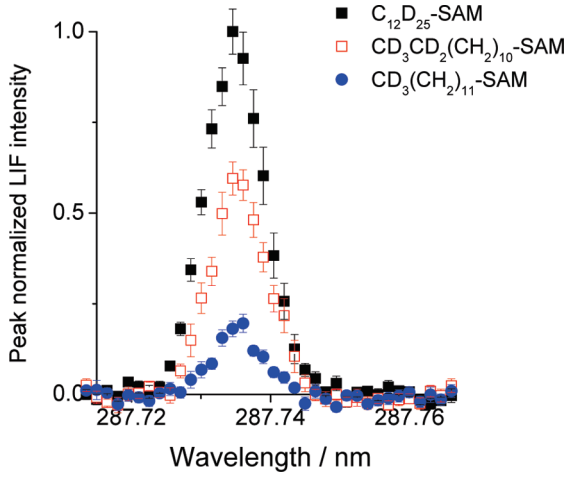

Figure 1. Early exposure (< 10 min; see text) OD A−X (1,0) $Q_1(1)$ LIF signals from $O(^3P)$ + partially and fully deuterated dodecyl SAMs. Signals are normalized to the $C_{12}D_{25}$ SAM. Photolysis probe delay = 11 μs. $p(NO_2)$ = 1 mTorr.

We concentrate here exclusively on the OD products. As expected from previous related work,[22−29,32] the appearance profiles as a function of the photolysis probe delay consisted of a characteristic "dead time" followed by a wave of OD returning from the surface. As for normal hydrogen or perdeutero SAMs,[32] these profiles contained a majority fast component consistent with a predominantly direct reaction mechanism. This observation also incidentally precludes the possibility that the SAM layers are covered with a substantial overlayer of adsorbed NO_2 through which the incoming $O(^3P)$ or outgoing OD would have to penetrate.

Figure 1 shows scans across an individual line ($Q_1(1)$) in the early exposure time (see below) OD LIF excitation spectra, recorded near the peak of the appearance profile (11 μs). Results are shown for each of the three dodecyl SAMs studied. On the assumption that the relative reactivities of the different sites on the alkyl chains are purely additive, neglecting for example possible complications from enhanced reactivity at domain boundaries, site-specific contributions can be deduced from the relative intensities of the LIF signals.

The numerical results of such repeated measurements are summarized in Table 1. The relatively modest yield from the terminal CD_3 group (which we label C_1 for the purposes of discussion) is deduced unambiguously from the $CD_3(CH_2)_{11}$ SAM alone. The difference between $CD_3(CH_2)_{11}$ and $CD_3CD_2(CH_2)_{10}$ SAMs indicates that the first secondary group (C_2) makes the single largest contribution. The remaining segments of the chain also contribute significantly though, given the further difference between the yields from the $CD_3CD_2(CH_2)_{10}$ and $C_{12}D_{25}$ SAMs. However, this contribution appears to be confined to C_3−C_6 because we also found that the yields from C_6D_{13} and $C_{12}D_{25}$ SAMs were the same within their errors. This suggests that beyond a critical chain length of ≤6 carbon atoms, either further CD_2 groups are inaccessible or else any OD produced is unable to escape. We had reached a similar conclusion previously using C_6H_{13} and $C_{18}H_{37}$ SAMs.[32]

In the conceptually related experiments of Jacobs and co-workers,[4−6] selectively deuterated dodecyl SAMs were bombarded with O^+ ions at much higher incident energies (5−40 eV or ∼500−4000 kJ mol^{-1}). On the basis of the observed OH^- ion production, it was inferred that H-abstraction was confined to the three outermost carbon atoms, as also indicated in Table 1.[5] The incoming O^+ ions are believed to be efficiently neutralized, so that the projectiles at the point of impact are $O(^3P)$ atoms, as here. It is not particularly surprising that the much higher energy atoms can react efficiently with the terminal methyl group. In our lower-energy experiments, reaction is clearly suppressed (despite stoichiometry favoring CD_3 over CD_2) by the higher barriers to abstraction from primary bonds.[36] It is much less obvious why the Jacobs experiments show minimal reactivity for C_3 and beyond, in contrast to ∼40 % of the total in our work. This could result from the much higher reactivity of the high-energy O atoms with the first group that they encounter. Such shielding of those at greater depths is likely to be a general phenomenon for highly reactive probes. Indeed, in recent theoretical modeling of the related, low-barrier reactions of F atoms with octyl SAMs, Layfield and Troya[37] predict that the great majority of the reactivity will be at the terminal CH_3 group.

Table 1. OD Production from Different Sites in Dodecyl SAMs

	contribution to OD detected	
carbon[a]	this work[b]	Jacobs[c]
C_1	(16 ± 3) %	> 75 %
C_2	(42 ± 5) %	∼20 %
C_3−C_6	(42 ± 4) %	< 2.5 %[d]
C_7−C_{12}	0 (< 4 %)[e]	

[a] Numbered from the terminal CD_3 group. [b] 2σ uncertainties from repeated measurements. [c] On the basis of the OD^- anion yield.[6] [d] C_3 only. [e] Upper bound based on uncertainties in the difference between C_6 and C_{12} SAM signals.

Alternatively, though, all such measurements represent a lower limit on penetration if the product can itself undergo secondary loss processes. Therefore, the discrepancies between our experiments and those of Jacobs could lie in different escape probabilities of the respective neutral and ionic products. Jacobs and co-workers had already reflected[5] on a possible bias for escape of anions to be confined to the outer layers of the surface. Ions formed at greater depths are presumably more likely to be slower moving and consequently less likely to escape without undergoing reverse electron transfer. In our own experiments, the neutral OH may also be lost through abstraction of a second H (or D) atom to form water, but apparently, this does not prevent the escape of a significant fraction of OD from sites at least as deep as C_3.

The closest available theory is hybrid quantum mechanical/molecular mechanical (QM/MM) calculations of $O(^3P)$ reactions with model SAMs.[33,34] The reactivity at different points along the chain was explored by Troya and Schatz,[34] but at much higher collision energies (5 eV). Their choice of initial conditions biased the collisions toward impacts on the ends of, rather than between, chains. They also did not fully explore the incoming polar and azimuthal angles (defined relative to the 30° tilt axis of the chains). Nevertheless, they demonstrated how C_1 and C_2 are exposed to direct attack

DOI: 10.1021/jz100587g | J. Phys. Chem. Lett. 2010, 1, 1917–1921

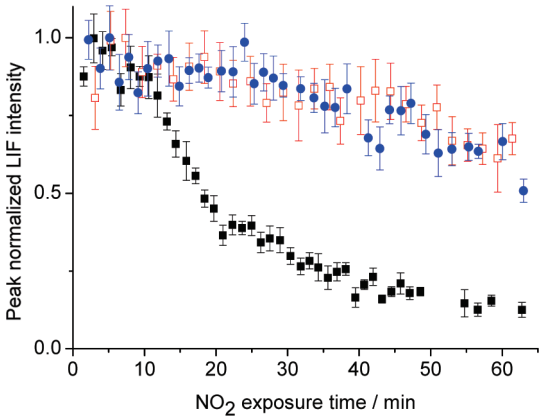

Figure 2. OD A−X (1,0) $Q_1(1)$ LIF signal decay as a function of exposure time to NO_2 (1 mTorr) from C_6D_{13} (black filled squares), $C_{12}D_{25}$ (red open squares), and $CD_3CD_2(CH_2)_{10}$ SAMs (blue filled circles). All traces have been normalized to their values at early times.

and how even C_3 and C_4 (the greatest depth allowed by their model) could be accessed relatively easily, in some cases following a nonreactive deflection from an outer group. In more recent work, Hase and co-workers[38] have explored the inelastic scattering of $O(^3P)$ from SAMs over a wide range of energies and polar angles and with randomly selected impact sites and azimuthal angles. They predicted a considerable probability for penetration at all collision energies. At the lowest energies studied (0.5 kJ mol^{-1}), the mechanism was an initial physisorption followed by migratory, shallow penetration. However, direct, ballistic penetration became increasingly important at higher energies more comparable to those in the current work. The average penetration depth was found to be a function of incident angle, in all cases continuing to increase monotonically with energy up to much higher values (500 kJ mol^{-1}) overlapping the lower end of the range in the Jacobs experiments.[4−6] Hase and co-workers[38] therefore speculated, very interestingly in light of our results, that a more complete reactive model might show enhanced abstraction at greater depths. Further reactive scattering calculations matching more closely the conditions of our experiments would clearly be of interest. These could address intriguing aspects not yet determined experimentally, especially the competition between escape and secondary reaction as a function of the depth at which OH is formed.

A key technical difference from reactive studies on liquid surfaces is that the SAM layer cannot easily be refreshed during a measurement. A secondary result of our work was therefore to determine the stability of SAMs exposed to NO_2. As shown in Figure 2, the OD yields were indeed found to drop over time. The stability of the shorter-chain C_6D_{13} SAM is considerably less than that of the dodecyl SAMs. We have established that the critical factor is exposure to NO_2, regardless of whether $O(^3P)$ atoms are being generated by photolysis. The C_6D_{13} SAM shows an induction period on the order of ∼10 min, during which the OD signal remains relatively constant, followed by a relatively rapid decline. Similar observations on undeuterated SAMs were the reason that we had restricted samples to a maximum 10 min exposure to

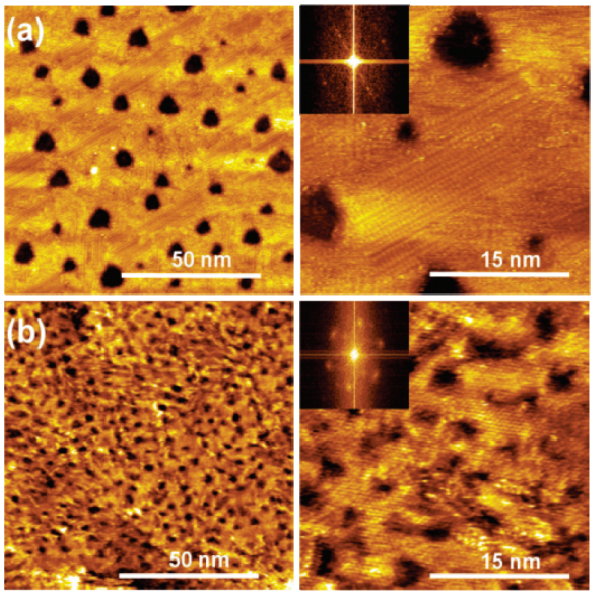

Figure 3. Low (left) and high (right) resolution STM images of thioalkyl SAMs of chain length (a) C_6 and (b) C_{12} following 10 min of NO_2 exposure (1 mTorr). Insets are fast Fourier transforms of the high-resolution images, showing typical hexagonal packing for the C_{12} sample but a lack of symmetry indicative of destruction for the C_6 SAM.

NO_2 in our previous preliminary study of SAM reactivity.[32] This does not guarantee that no changes are taking place on the surface during that period, as we address more directly below. More reassuringly, we have established here that for the longer-chain SAMs, the OD signal decay was much less pronounced. More than 60% of the OD signal was retained after an exposure period of ∼1 h. Interestingly, the shape of the decay curve is independent of the extent of deuteration. This is consistent with the loss mechanism being the detachment of intact chains, rather than stepwise erosion beginning at the outermost segments.

We have examined the mechanism for SAM damage through more detailed STM measurements. These confirm that only the shorter-chain (C_6) SAMs are significantly damaged during the early-time exposure to NO_2. In Figure 3, we show high-resolution STM images of the C_6 (fully deuterated) and C_{12} (undeuterated) surfaces following 10 min of exposure to NO_2. On both surfaces, there are gold vacancy islands that are characteristic of thiol SAMs. The C_{12} SAM surface is indistinguishable from that of a sample prior to NO_2 exposure (see Supporting Information). The C_{12} molecules have maintained their hexagonal arrangement and upright orientation. In contrast, on the exposed C_6 surface, there is now less than a monolayer of molecules, as evidenced by the striped features in Figure 3a, which are indicative of flat-lying molecules. The deterioration of this SAM is also reflected in the lower density and larger area of the vacancy islands because of the consequential higher mobility of Au atoms.

Previous studies have shown that atomic oxygen or ozone in ambient air[39,40] can damage SAMs, but this is, to our knowledge, the first identification that NO_2 is also capable of damaging thiol SAMs. The STM results support the conclusion from

DOI: 10.1021/jz100587g | J. Phys. Chem. Lett. 2010, 1, 1917–1921

the OD LIF decays that the mechanism for SAM destruction is stripping of the surface by detachment of entire chains through breaking of the S—Au bond, consistent with a higher probability of NO_2 molecules penetrating to the base for shorter-chain SAMs.

EXPERIMENTAL SECTION

Two partially deuterated ($CD_3(CH_2)_{11}SH$ and $CD_3CD_2(CH_2)_{10}SH$) thiols were synthesized and prepared as described in the Supporting Information. Two commercial fully deuterated ($C_6D_{13}SH$ and $C_{12}D_{25}SH$) thiols were also used. The corresponding commercial C_6 and C_{12} undeuterated thiols were used for some of the supporting STM measurements. SAMs were prepared on Au(111)-coated mica slides and characterized by scanning tunneling microscopy as described in the Supporting Information. Otherwise, the core experimental method was similar to that previously applied successfully to reactions of $O(^3P)$ with liquids[22−29] and in a preliminary study with SAMs.[32] Further details of the laser-based approach are also provided in the Supporting Information. In essence, superthermal $O(^3P)$ atoms were generated by 355 nm laser photolysis[35] of a carefully controlled low pressure (nominally 1 mTorr) of NO_2 gas. The SAM surfaces were held at 6 mm from this laser axis. A fraction of the OD $X^2\Pi$ radicals generated are detected by LIF using a second, tunable laser beam at the same distance from the surface.

SUPPORTING INFORMATION AVAILABLE Synthesis of deuterated thiols; preparation and characterization of SAMs; experimental apparatus. This material is available free of charge via the Internet at http://pubs.acs.org.

AUTHOR INFORMATION

Corresponding Author:

*To whom correspondence should be addressed. E-mail: k.g.mckendrick@hw.ac.uk.

ACKNOWLEDGMENT Claire Schmitt contributed to the LIF experiments. M.L.C. was supported by an RCUK Academic Fellowship. We acknowledge a research grant from EPSRC.

REFERENCES

(1) Paz, Y.; Trakhtenberg, S.; Naaman, R. Destruction of Organized Organic Monolayers by Oxygen-Atoms. *J. Phys. Chem.* **1992,** *96*, 10964–10967.

(2) Paz, Y.; Trakhtenberg, S.; Naaman, R. Reaction Between $O(^3P)$ and Organized Organic Thin-Films. *J. Phys. Chem.* **1994,** *98*, 13517–13523.

(3) Wagner, A. J.; Wolfe, G. M.; Fairbrother, D. H. Atomic Oxygen Reactions with Semifluorinated and n-Alkanethiolate Self-Assembled Monolayers. *J. Chem. Phys.* **2004,** *120*, 3799–3810.

(4) Qin, X. D.; Tzvetkov, T.; Jacobs, D. C. Reaction of 5 eV O^+ with a Decanethiolate/Au(111) Self-Assembled Monolayer. *Nucl. Instrum. Methods Phys. Res., Sect. B* **2003,** *203*, 130–135.

(5) Qin, X. D.; Tzvetkov, T.; Liu, X.; Lee, D. C.; Yu, L. P.; Jacobs, D. C. Site-Selective Abstraction in the Reaction of 5−20 eV O^+ with a Self-Assembled Monolayer. *J. Am. Chem. Soc.* **2004,** *126*, 13232–13233.

(6) Qin, X. D.; Tzvetkov, T.; Jacobs, D. C. Reaction of 5−40 eV Ions with Self-Assembled Monolayers. *J. Phys. Chem. A* **2006,** *110*, 1408–1415.

(7) Isa, N.; Gibson, K. D.; Yan, T.; Hase, W. L.; Sibener, S. J. Experimental and Simulation Study of Neon Collision Dynamics with a 1-Decanethiol Monolayer. *J. Chem. Phys.* **2004,** *120*, 2417–2433.

(8) Day, B. S.; Davis, G. M.; Morris, J. R. The Effect of Hydrogen-Bonding and Terminal Group Structure on the Dynamics of Ar Collisions with Self-Assembled Monolayers. *Anal. Chim. Acta* **2003,** *496*, 249–258.

(9) Day, B. S.; Morris, J. R. Even—Odd Orientation and Chain-Length Effects in the Energy Exchange of Argon Collisions with Self-Assembled Monolayers. *J. Phys. Chem. B* **2003,** *107*, 7120–7125.

(10) Day, B. S.; Shuler, S. F.; Ducre, A.; Morris, J. R. The Dynamics of Gas-Surface Energy Exchange in Collisions of Ar Atoms with Omega-Functionalized Self-Assembled Monolayers. *J. Chem. Phys.* **2003,** *119*, 8084–8096.

(11) Lohr, J. R.; Day, B. S.; Morris, J. R. Dynamics of HCl collisions with Hydroxyl- and Methyl-Terminated Self-Assembled Monolayers. *J. Phys. Chem. A* **2006,** *110*, 1645–1649.

(12) Alexander, W. A.; Day, B. S.; Moore, H. J.; Lee, T. R.; Morris, J. R.; Troya, D. Experimental and Theoretical Studies of the Effect of Mass on the Dynamics of Gas/Organic-Surface Energy Transfer. *J. Chem. Phys.* **2008,** *128*, 014713.

(13) Saecker, M. E.; Govoni, S. T.; Kowalski, D. V.; King, M. E.; Nathanson, G. M. Molecular-Beam Scattering from Liquid Surfaces. *Science* **1991,** *252*, 1421–1424.

(14) Nathanson, G. M. Molecular Beam Studies of Gas—Liquid Interfaces. *Annu. Rev. Phys. Chem.* **2004,** *55*, 231–255.

(15) Yan, T. Y.; Hase, W. L.; Barker, J. R. Identifying Trapping Desorption in Gas—Surface Scattering. *Chem. Phys. Lett.* **2000,** *329*, 84–91.

(16) Tasic, U.; Day, B. S.; Yan, T. Y.; Morris, J. R.; Hase, W. L. Chemical Dynamics Study of Intrasurface Hydrogen-Bonding Effects in Gas—Surface Energy Exchange and Accommodation. *J. Phys. Chem. C* **2008,** *112*, 476–490.

(17) Garton, D. J.; Minton, T. K.; Alagia, M.; Balucani, N.; Casavecchia, P.; Volpi, G. G. Reactive Scattering of Ground-State and Electronically Excited Oxygen Atoms on a Liquid Hydrocarbon Surface. *Faraday Discuss.* **1997,** *108*, 387–399.

(18) Garton, D. J.; Minton, T. K.; Alagia, M.; Balucani, N.; Casavecchia, P.; Volpi, G. G. Comparative Dynamics of $Cl(^2P)$ and $O(^3P)$ Interactions with a Hydrocarbon Surface. *J. Chem. Phys.* **2000,** *112*, 5975–5984.

(19) Garton, D. J.; Minton, T. K.; Alagia, M.; Balucani, N.; Casevecchia, P.; Volpi, G. G. Erratum: "Comparative Dynamics of $Cl(^2P)$ and $O(^3P)$ Interactions with a Hydrocarbon Surface". *J. Chem. Phys.* **2001,** *114*, 5958.

(20) Zhang, J. M.; Garton, D. J.; Minton, T. K. Reactive and Inelastic Scattering Dynamics of Hyperthermal Oxygen Atoms on a Saturated Hydrocarbon Surface. *J. Chem. Phys.* **2002,** *117*, 6239–6251.

(21) Zhang, J. M.; Upadhyaya, H. P.; Brunsvold, A. L.; Minton, T. K. Hyperthermal Reactions of O and O_2 with a Hydrocarbon Surface: Direct C—C Bond Breakage by O and H-Atom Abstraction by O_2. *J. Phys. Chem. B* **2006,** *110*, 12500–12511.

(22) Kelso, H.; Kohler, S. P. K.; Henderson, D. A.; McKendrick, K. G. Dynamics of the Gas—Liquid Interfacial Reaction of $O(^3P)$ Atoms with Hydrocarbons. *J. Chem. Phys.* **2003,** *119*, 9985–9988.

DOI: 10.1021/jz100587g | *J. Phys. Chem. Lett.* **2010,** *1*, 1917–1921

(23) Kohler, S. P. K.; Allan, M.; Kelso, H.; Henderson, D. A.; McKendrick, K. G. The Effects of Surface Temperature on the Gas−Liquid Interfacial Reaction Dynamics of O(^{3}P) plus Squalane. *J. Chem. Phys.* **2005,** *122*, 024712.

(24) Kohler, S. P. K.; Allan, M.; Costen, M. L.; McKendrick, K. G. Direct Gas−Liquid Interfacial Dynamics: The Reaction Between O(^{3}P) and a Liquid Hydrocarbon. *J. Phys. Chem. B* **2006,** *110*, 2771–2776.

(25) Allan, M.; Bagot, P. A. J.; Kohler, S. P. K.; Reed, S. K.; Westacott, R. E.; Costen, M. L.; McKendrick, K. G. Dynamics of Interfacial Reactions Between O(^{3}P) Atoms and Long-Chain Liquid Hydrocarbons. *Phys. Scr.* **2007,** *76*, C42–C47.

(26) Allan, M.; Bagot, P. A. J.; Costen, M. L.; McKendrick, K. G. Temperature Dependence of OH Yield, Translational Energy, and Vibrational Branching in the Reaction of O(^{3}P)(g) with Liquid Squalane. *J. Phys. Chem. C* **2007,** *111*, 14833–14842.

(27) Allan, M.; Bagot, P. A. J.; Westacott, R. E.; Costen, M. L.; McKendrick, K. G. Influence of Molecular and Supramolecular Structure on the Gas−Liquid Interfacial Reactivity of Hydrocarbon Liquids with O(^{3}P) Atoms. *J. Phys. Chem. C* **2008,** *112*, 1524–1532.

(28) Waring, C.; Bagot, P. A. J.; Slattery, J. M.; Costen, M. L.; McKendrick, K. G. O(^{3}P) Atoms as a Probe of Surface Ordering in 1-Alkyl-3-methylimidazolium-Based Ionic Liquids. *J. Phys. Chem. Lett.* **2010,** *1*, 429–433.

(29) Waring, C.; Bagot, P. A. J.; Slattery, J. M.; Costen, M. L.; McKendrick, K. G. O(^{3}P) Atoms as a Chemical Probe of Surface Ordering in Ionic Liquids. *J. Phys. Chem. A* **2010,** *114*, 4896–4904.

(30) Zolot, A. M.; Harper, W. W.; Perkins, B. G.; Dagdigian, P. J.; Nesbitt, D. J. Quantum-State Resolved Reaction Dynamics at the Gas-Liquid Interface: Direct Absorption Detection of HF(v,J) Product from F(^{2}P) Plus Squalane. *J. Chem. Phys.* **2006,** *125*, 021101.

(31) Zolot, A. M.; Dagdigian, P. J.; Nesbitt, D. J. Quantum-State Resolved Reactive Scattering at the Gas−Liquid Interface: F+Squalane ($C_{30}H_{62}$) Dynamics via High-Resolution Infrared Absorption of Nascent HF(v,J). *J. Chem. Phys.* **2008,** *129*, 194705.

(32) Waring, C.; Bagot, P. A. J.; Räisänen, M. T.; Costen, M. L.; McKendrick, K. G. Dynamics of the Reaction of O(^{3}P) Atoms with Alkylthiol Self-Assembled Monolayers. *J. Phys. Chem. A* **2009,** *113*, 4320–4329.

(33) Li, G.; Bosio, S. B. M.; Hase, W. L. A QM/MM model for O(^{3}P) Reaction with an Alkyl Thiolate Self-Assembled Monolayer. *J. Mol. Struct.* **2000,** *556*, 43–57.

(34) Troya, D.; Schatz, G. C. Theoretical Studies of Hyperthermal O(^{3}P) Collisions with Hydrocarbon Self-Assembled Monolayers. *J. Chem. Phys.* **2004,** *120*, 7696–7707.

(35) Baker, R. P.; Costen, M. L.; Hancock, G.; Ritchie, G. A. D.; Summerfield, D. Vector Correlations in the 355 nm Photolysis of Thermal NO_2. *Phys. Chem. Chem. Phys.* **2000,** *2*, 661–664.

(36) Ausfelder, F.; McKendrick, K. G. The Dynamics of Reactions of O(^{3}P) Atoms with Saturated Hydrocarbons and Related Compounds. *Prog. React. Kinet. Mech.* **2000,** *25*, 299–370.

(37) Layfield, J. P.; Troya, D. Theoretical Study of the Dynamics of F+Alkanethiol Self-Assembled Monolayer Hydrogen-Abstraction Reactions. *J. Chem. Phys.* **2010,** *132*, 134307.

(38) Tasic, U. S.; Yan, T. Y.; Hase, W. L. Dynamics of Energy Transfer in Collisions of O(^{3}P) Atoms with a 1-Decanethiol Self-Assembled Monolayer Surface. *J. Phys. Chem. B* **2006,** *110*, 11863–11877.

(39) Schoenfisch, M. H.; Pemberton, J. E. Air Stability of Alkanethiol Self-Assembled Monolayers on Silver and Gold Surfaces. *J. Am. Chem. Soc.* **1998,** *120*, 4502–4513.

(40) Willey, T. M.; Vance, A. L.; van Buuren, T.; Bostedt, C.; Terminello, L. J.; Fadley, C. S. Rapid Degradation of Alkanethiol-Based Self-Assembled Monolayers on Gold in Ambient Laboratory Conditions. *Surf. Sci.* **2005,** *576*, 188–196.

DOI: 10.1021/jz100587g | *J. Phys. Chem. Lett.* **2010,** *1*, 1917–1921